

Simulation of Self-Piercing Riveting Process and Joint Failure with focus on Material Damage and Failure modelling

Aman Rusia^{1,2}, Dr. Markus Beck¹, Prof.-Dr. Stefan Weihe²

¹Daimler AG, Stuttgart (DE)

²Materialprüfungsanstalt (MPA), University of Stuttgart, Stuttgart (DE)

1 Introduction

Weight reduction is one of the main objectives that has played a pivotal role in designing Automobiles in the past decades. Various methods can be employed in this direction such as replacing traditional steel with lightweight aluminum alloys or using a combination of multiple lightweight materials. Joining techniques like spot welding, which generally perform well for joining of steel body panels, do not yield satisfactory results in joining of aluminum sheets. Consequently, there has been an increasing interest in developing alternative joining techniques as a replacement for spot welding in the automotive industry.

One of the relatively new techniques used intensively nowadays is the Self Piercing Riveting (SPR). In principle, it is a cold forming process in which a semi-tubular rivet is pressed by a plunger so that it pierces through the thickness of the top sheet and flares in the bottom sheet, thereby forming a mechanical interlock. With an increased usage of the self-piercing rivets, the demand for understanding the mechanical behavior of such joints is also on the rise. Numerical simulation is a very effective way of shortening the production cycle by replacing time-consuming experiments with computer simulation.

However, estimating the failure of SPR joints becomes very challenging because it is preceded by high localized deformation and/or complete fracture of one or more joined sheets. Therefore, proper modelling of damage and failure in the materials is necessary for an accurate prediction of the SPR joint failure. In this paper a thorough scheme is presented to accurately perform the joint failure analysis of the self-piercing rivet connections, taking into account the damage and failure in the associated materials. Presently the study is being done with 2-sheet SPR joints only which can be extended to 3-sheet joints in future.

2 Theory and Motivation

2.1 Self-Piercing Riveting

2.1.1 Joining Process

Self-Piercing Riveting (SPR) is a mechanical joining technique involving a cold-forming process in which a semi-tubular rivet is used to join two or more sheet materials together. The entire SPR process can be described in the following four steps [1] (Figure 1):

- Clamping: In this step, the blank holder presses the sheets to be joined against the die. The required clamping force depends on the number and strength of the sheets to be joined.

- Piercing: By lowering the punch, the rivet is pressed into the punch side sheet. The rivet cuts through the sheet. The duration of this step depends on the material of the sheets to be joined and on the rivet material.

- Flaring: During this step, the rivet is further punched and bent in the workpiece to produce an undercut in the die-side sheet. The deformation of the rivet essentially depends on the shape of die, and the strength of rivet and sheets involved in the joint.

- Release: After the punch has reached a certain pre-defined force or stroke, it returns to its initial position and the finished joint is removed from the die.

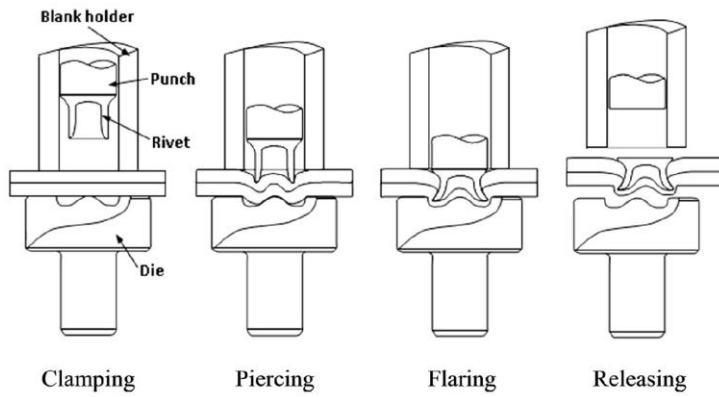


Fig.1: Schematic description of Self-Piercing Riveting Process [1]

2.1.2 Joint Strength Evaluation

The strength of an SPR joint depends on many factors, such as, the strength and thickness of the joined sheets, the amount of undercut, the final position of rivet head after joining, etc. Various types of specimens are available to test the joint strength under various loading conditions, such as e.g. U-shaped specimen, peel specimen, shear specimen, etc. (Figure 2 and 3).

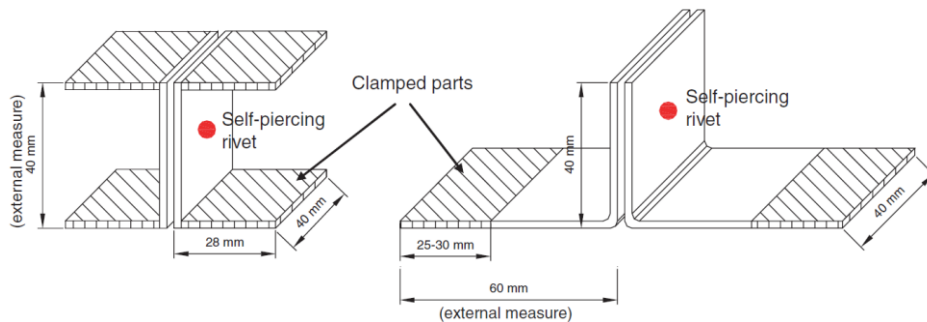


Fig.2: U-shaped (left) und Peel (right) specimen [2]

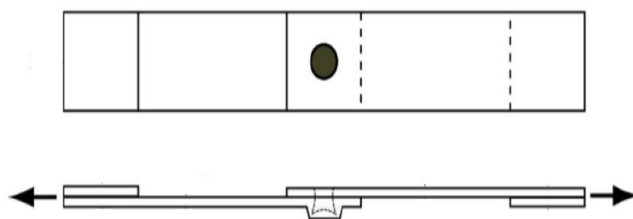


Fig.3: Shear Specimen [3]

The SPR joint failure involves movement of rivet through the thickness of sheet materials which leads to severe localized deformation in sheets. The fracture in one (or both) of the sheet(s) can also be a potential reason for failure of the joint. The typical modes of failure in SPR joints can be categorized under 3 variants:

- Single sided deformation mode (V1): In this mode of failure, the rivet is pulled out of either top or bottom sheet leading to small or large deformation in either one of the sheet materials.
- Single sided fracture mode (V2): In this mode of failure, the rivet is pulled out of either top or bottom sheet leading to partial or complete fracture in either one of the sheet materials.
- Mixed mode (V3): In this mode of failure, the rivet is pulled out of either one or both sheet(s) leading to deformation or fracture in both of the sheet materials.



Fig.4: SPR joint failure modes, (from left to right) V1, V2, V3

As the sheet materials are plastically deformed during joint failure tests which sometimes leads to fracture in the material, the damage and failure modeling of materials plays a special role in prediction of joint failure through simulations. The material damage/failure models are discussed in Section 2.2.

2.2 Material Damage and Failure modelling

In the last half century, there have been numerous attempts to study and model the phenomenon of ductile fracture. Various numerical damage and failure models have been developed to support the finite element simulations of different processes covering a broad range of materials. These models can be broadly classified into two categories: micromechanical models and macromechanical (also known as phenomenological) models. The macromechanical models are further classified into two categories: coupled and uncoupled models. Further description of damage and failure models has been provided in the following sub-sections.

2.2.1 Micromechanical models

The microstructure of metals and engineering alloys is very complex and although on a macroscopic level we can assume that the material is homogeneous, from microscopic point of view a material is considered as a cluster of inhomogeneous particles. In micromechanical approach of material modelling, these particles are collectively considered as voids. Ductile fracture in this case is defined as material separation which is a result of microscopic damage accumulation. This is a complicated phenomenon that starts with nucleation, growth and coalescence of voids found in the material (Figure 5).

Some examples of micromechanical models are: Gurson/Gurson-Tvergaard-Needleman (GTN), McClintock, etc.

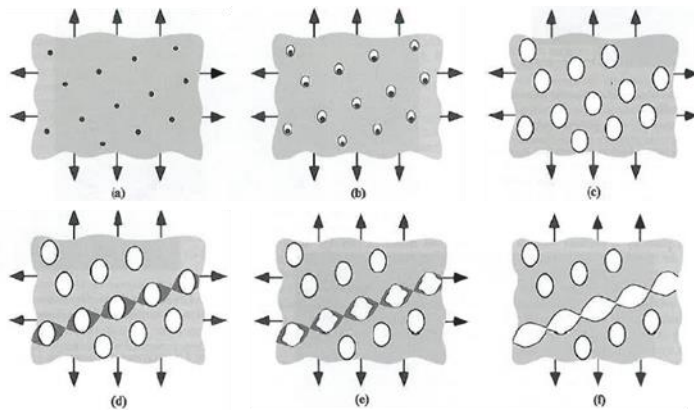


Fig.5: Illustrative description of the micromechanical failure approach [4]

2.2.2 Macromechanical models

These models are based on macroscopic field variables such as stress tensor, strain tensor, etc. [6]. For each of the models, different "Damage" parameters are proposed that quantify the actual damage associated with material deformation on an aggregate level.

In case of "uncoupled" macromechanical models, the aggregation of damage has no impact on the material properties. Therefore, these models are not capable of estimating the softening of the material after necking phenomenon. However, in case of "coupled" macromechanical models, the damage variable has a direct impact on the material behaviour under loading. Therefore, a damage induced material softening can be observed in such models after necking.

The uncoupled models can also be simply referred as material failure models and coupled models can be referred as material damage models. The difference between coupled and uncoupled models is shown in Figure 6.

Some examples of macromechanical models are: Johnson-Cook, Lemaitre, GISSMO (Generalised Incremental Stress State dependent damage MOdel), etc.

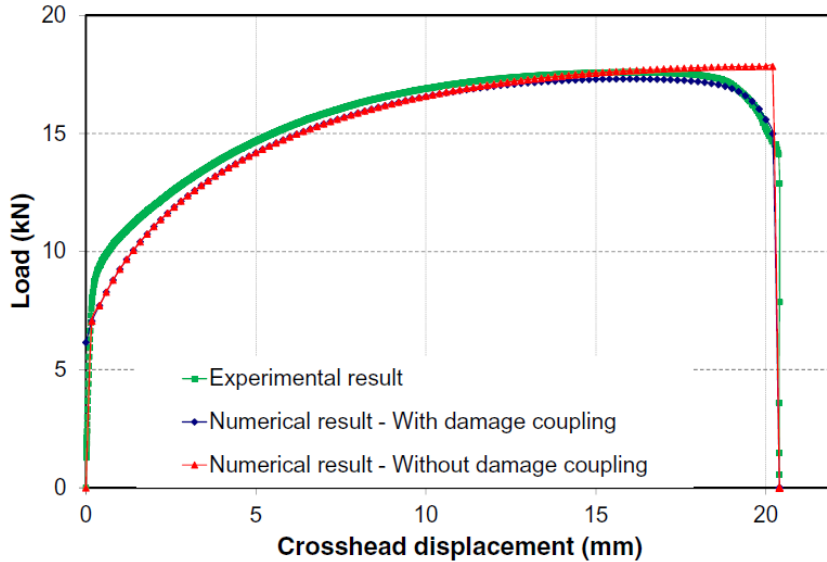


Fig.6: Difference between “coupled” and “uncoupled” macromechanical models [5]

2.3 Stress-state dependence of Damage/Failure models

It is important to understand the dependence of the material damage and failure models on the two stress-state related parameters: Stress Triaxiality (η) and Lode parameter (ξ), as they directly influence the material ductility. The stress triaxiality is measured as the ratio of mean stress and equivalent stress while Lode parameter is related with normalized third deviatoric stress invariant [7]. The material failure can be described in terms of failure strains which are further dependent on the stress-state of material at any particular instant.

Based on their application in finite element models and dependence on stress-state parameters, the damage/failure models can be classified into 2D and 3D material models. The distinction between these models is explained in the following sub-sections.

2.3.1 2D material failure models

These material damage/failure models find their applicability in the finite element models with shell elements. These material models depend only on stress triaxiality to define the failure strains and the relationship can be described in the form of a failure curve. For shell elements, the numerical value of triaxiality varies in the range of $-1 \leq \eta \leq +1$, with -1 being the biaxial compression, 0 being the shear and $+1$ being the biaxial tensile stress state. An example of failure curve is shown in Figure 7(a).

2.3.2 3D material failure models

These material damage/failure models are applicable in finite element models with solid elements. The definition of failure strains in these material models is a function of both stress triaxiality and Lode parameter and their relationship can be described in the form of a failure surface. In case of solid elements, the numerical value of triaxiality varies in the range of $-\infty \leq \eta \leq +\infty$, with $-\infty$ being the hydrostatic compression, 0 being the shear and $+\infty$ being the hydrostatic tensile stress state. The numerical value of Lode parameter lies in the range of $-1 \leq \xi \leq +1$, with -1 being axisymmetric compression, 0 being generalized shear and $+1$ being the axisymmetric tensile stress state. An example of failure surface is shown in Figure 7(b).

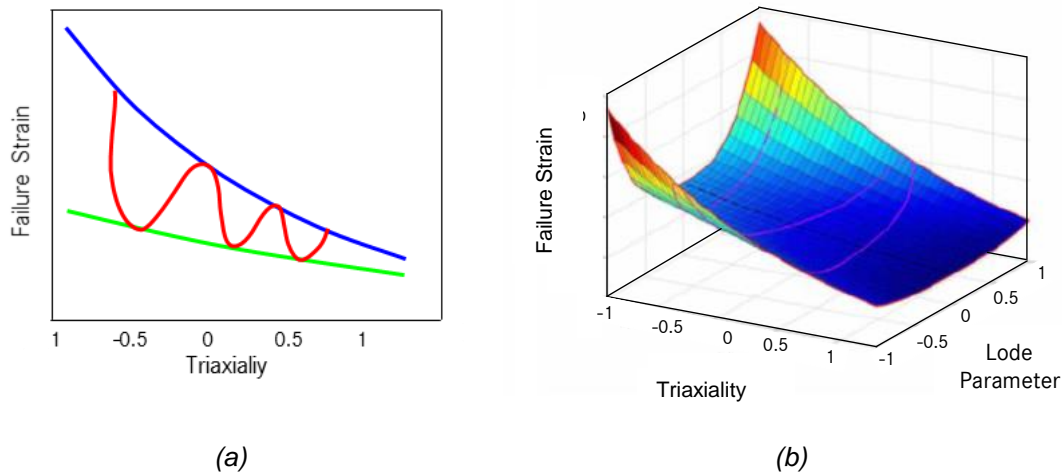


Fig.7: (a) 2D model: Failure curve (red), (b) 3D model: Failure Surface [8]

3 Identification and Modelling of material damage models

A number of options are available for material damage models (both micro- and macromechanical) which can be considered for simulations to evaluate the joint strength of a SPR connection. A systematic study was planned to evaluate some of these models using LS-DYNA as the numerical solver.

3.1 Identification of damage models

Multiple options were available for micromechanical models which can be used for joint failure simulation, however, since the Gurson/GTN model [9] [10] was readily available from the crash simulation database for most of the materials, it was preferred for initial investigations. Similarly, in case of macromechanical models, GISSMO (Generalized Incremental Stress State dependent damage MOdel) [11] [12] [13] was available in the crash simulation database for a number of materials and can also be used readily as per availability. Although these material models from database are 2D damage models calibrated for shell elements, they provide a good basis for initial investigations with detailed joint failure simulation models with solid elements.

For detailed investigations the 3D damage models can be used to get a more accurate response to deformation in solid elements. A number of different models were studied based on their extent of applicability, dependence on Lode Parameter, number of input parameters required, etc. and three models were selected to be calibrated as 3D damage models using experimental results. The selected models were: Wilkins [14], Xue-Wierzbicki [15] [16] [17] and Modified Mohr-Coulomb [18] [19] model. The experimental program and calibration details are provided in Section 5.

3.2 Modelling method

Although there are many pre-defined material cards offered by LS-DYNA specific to particular material models, e.g. Gurson (MAT_120), Johnson Cook (MAT_015), etc. [20], there are also a number of material models which are unavailable as standard material cards. To use these material models in LS-DYNA, the creation of a “user-defined” material model is required, which can be a time consuming task and requires considerable effort.

A new approach is proposed in this study which employs GISSMO as a common framework for all macromechanical models (both 2D and 3D) which employs a damage parameter and failure curve/surface to describe the material behaviour. The GISSMO, being a generalized model, provides the user a unique opportunity to control parameters like damage coefficient and failure curve/surface to be fitted into any particular material damage/failure model. The failure curve/surface can be generated using experimental data for any desired material model based on the associated empirical equations. This provides the user flexibility and convenience to perform investigations with a number of material models which are currently unavailable as standard material cards in LS-DYNA.

4 Simulation Process Chain

An important thing to consider is that the joining process for SPR is axisymmetric in nature about the central axis. However, the failure of the SPR joints is not axisymmetric. This analysis allows to save computational costs by considering only a 2D axisymmetric model for the process simulation and a 3D simulation model with shell-solid interaction for the joint failure simulation. Thus, the complete analysis for the SPR joint can be divided into five steps:

1. Process simulation: To accurately predict the joint geometry and stresses and strains in the region around the joint. Adaptive Remeshing is included to avoid any element distortions.
2. Springback analysis and Mesh coarsening: To predict the deformation of joint after the removal of forces and increase the mesh size for the 3D simulation model for joint failure analysis.
3. Geometry conversion and Mapping: To create a detailed 3D simulation model with the stresses and strains mapped from the 2D axisymmetric model after springback which ensures the inclusion of any strain hardening effects from joining process
4. Shell-Solid Interaction: To prepare different specimen geometries required for different loading conditions. A shell-solid hybrid model offers a more efficient simulation by reducing computation time.
5. Joint failure simulation: To predict the behaviour of the joint under different loading conditions.

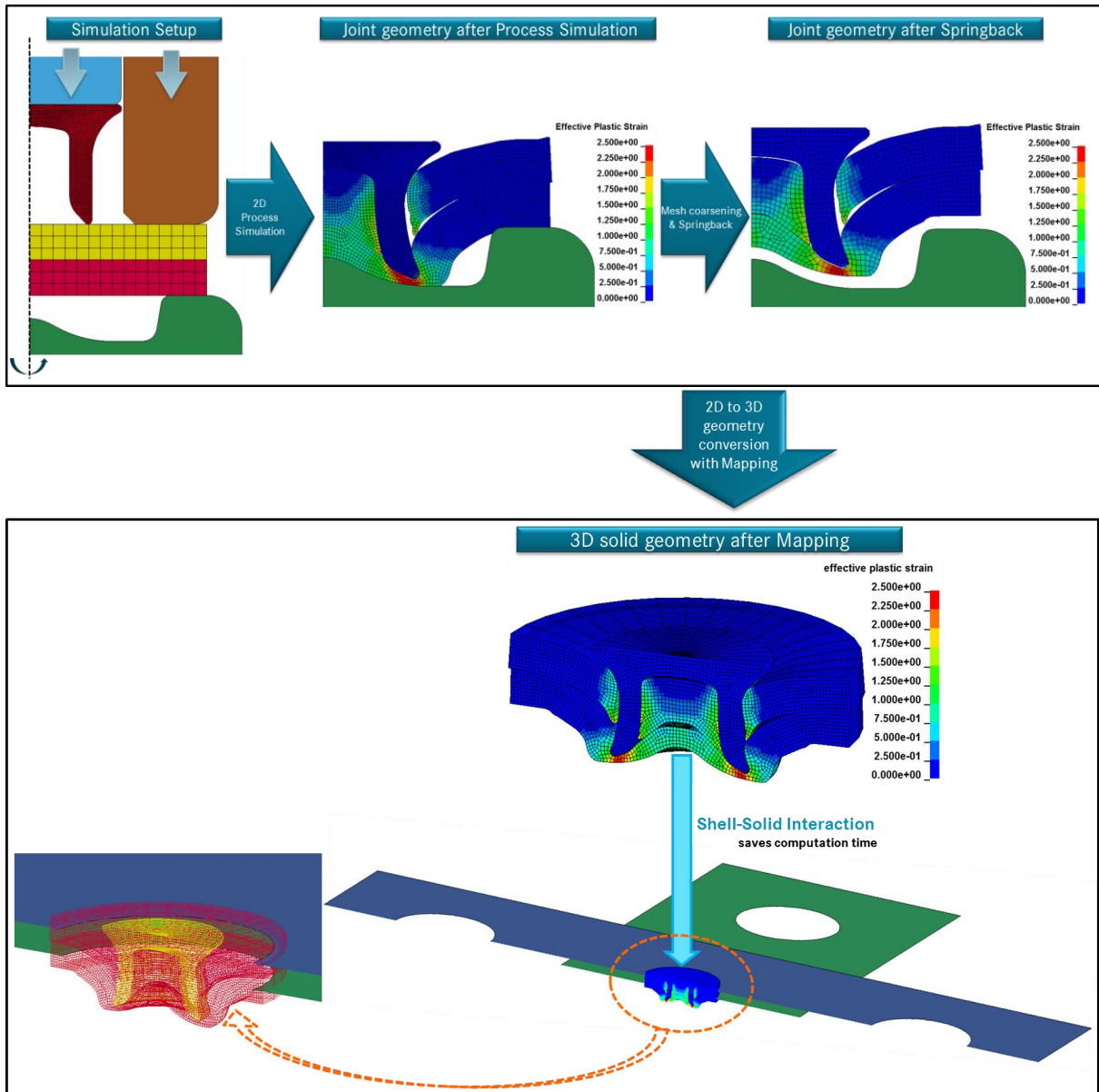


Fig.8: Description of simulation process chain

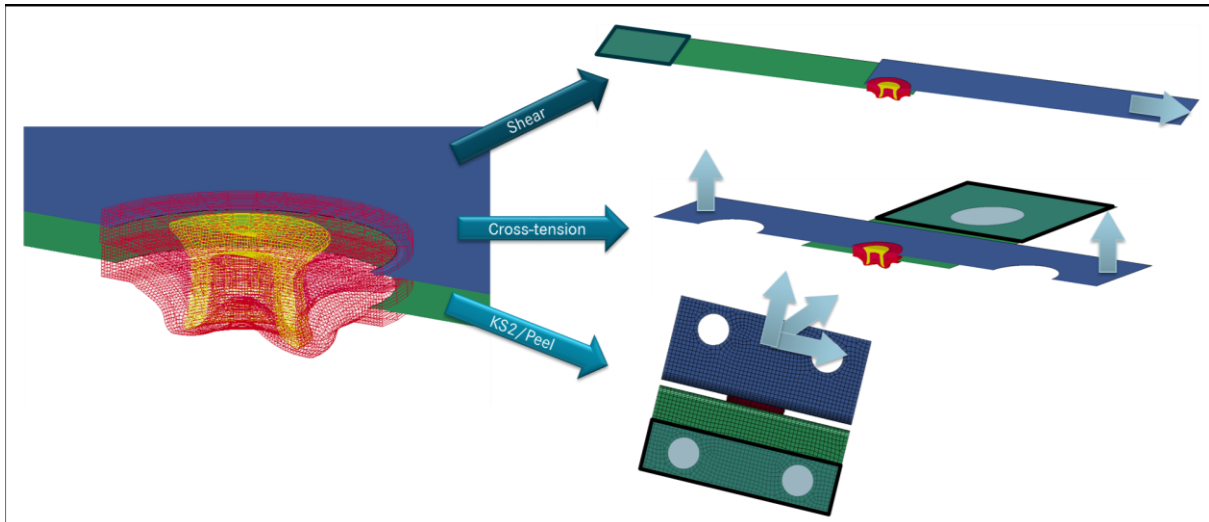


Fig.9: FE models for joint failure simulations with respective boundary conditions

LS-DYNA is used as the numerical solver for both joining process and joint failure simulations. The geometry conversion from 2D to 3D is performed by using LS-PREPOST and the mapping of stresses and strains is done by using a Python script. The shell-solid interaction is achieved by manually positioning the shell outer parts to get an overlap with solid inner parts and merging the nodes between shell and solid parts in the overlap region. The overlap is necessary to ensure the proper transfer of translational motion and bending moments from shells to solids and vice versa. The schematic representation of complete process chain can be seen in Figure 8 and 9.

5 Experimental and Numerical Investigations

For the purpose of this study, SPR joint made of 2.0 mm thick Aluminum 5xxx series top sheet and 2.5 mm thick Cast Aluminum as bottom sheet was considered. A steel rivet with dimensions 5 mm (nominal diameter) x 6 mm (length) was used for the riveting process. The description of the deformable parts is given in Table 1:

Part	Geometry	Material
Top sheet	2.0 mm (thickness)	AL 5xxx
Bottom sheet	2.5 mm (thickness)	Cast AL
Rivet	5x6 mm	H4

Table 1: Description of deformable parts from material combination

A 2D axisymmetric process simulation was performed for this material combination using the above mentioned rivet and 3 different die geometries to find an optimum rivet-die combination. Applying the methodology of simulation process chain mentioned in previous section, the initial joint failure simulations were performed with 2D damage models available from Crash simulation database. In the initial simulations mode of joint failure was found to be V1 (single sided deformation mode) with the rivet coming out of the bottom sheet causing high deformation in the sheet. This prognosis also matched well with the experimental results. However, the joint failure forces from the initial simulations were not entirely accurate and the deformation pattern in the bottom sheet was found different than the experiments. Hence, it was decided to perform numerical investigations with 3D damage models to find their effect on accuracy of prognosis. The calibration of 3D damage models was performed through a detailed experimental program described in the next sub-section.

5.1 Experimental Program

In the previous sections, several damage/failure models were discussed and 3 models were selected to be calibrated as 3D damage models. The calibration of 3D damage models includes a failure surface, i.e. failure strains as function of stress triaxiality and Lode parameter. Additionally, there are parameters that need to be calibrated to refine the damage prediction in the material.

Keeping in mind the prognosis from initial joint failure simulations with 2D damage models, the calibration of 3D damage models was performed primarily for the bottom sheet material, i.e. 2.5 mm thick Cast Aluminum.

For the calibration of the damage models, it is necessary to choose experiments that cover a wide range of stress triaxiality and Lode parameter values. Inspired by the works of Xue [6], T. Wierzbicki [21] and Zhuang [22], five experiments were planned for the bottom sheet material. The experiment specimens differ in their geometry to describe different stress states, as seen in Figure 10. The stress triaxiality, Lode parameter, and failure strain values for each specimen are mentioned in Table 2.

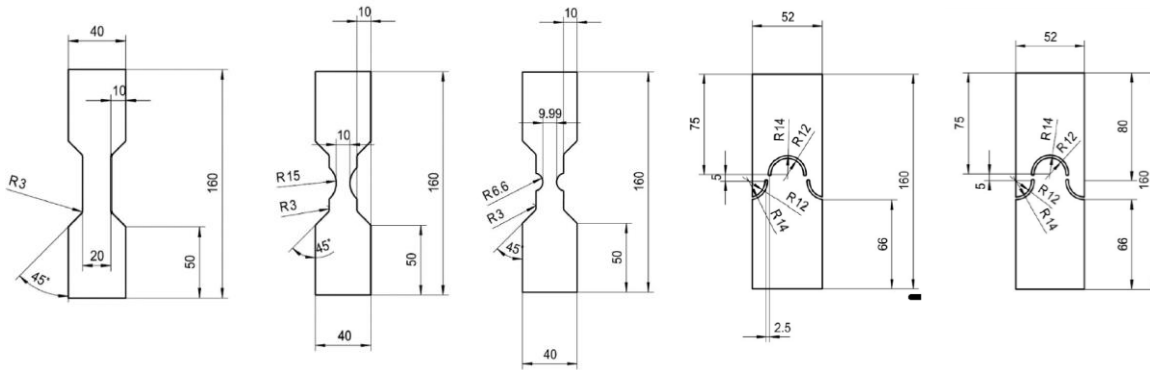


Fig.10: Specimen geometries, (from left to right) Unnotched, Notched I, Notched II, Shear I & Shear II

Specimen	Lode Parameter	Triaxiality	Failure strain
Unnotched	1.0	0.33	0.195
Notched I	0.9	0.45	0.190
Notched II	0.8	0.49	0.225
Shear I	0.86	0.39	0.280
Shear II	0.20	0.17	0.420

Table 2: Description of specimen related experimental data

5.2 Calibration of failure surfaces

For the calibration of failure surface, an optimization algorithm was written on MATLAB to find the required parameter values. In this optimization algorithm, an iterative method was employed using *fminsearch* operation to minimize the multivariable objective function which in this case was the mean squared error (MSE) between the numerical failure strain and experimental failure strain [23]. For such an optimization algorithm, it is necessary to use at least as many experimental results as the number of unknown variables in the constitutive equation of the damage model. Based on the number of unknown variables for Wilkins, Xue-Wierzbicki and Modified Mohr-Coulomb, the required minimum experiments are 4, 4 and 2 respectively.

In the initial joint failure simulations, it was also found that some elements also fail in the negative triaxiality region (compression) and therefore, an additional failure strain with high numerical value of 3.5 for triaxiality -2.0 and Lode parameter -0.9 was added to the MATLAB input data set for calibration of failure surface of each damage model. This approximate value was generated by simulating an indentation test with the available 2D GISSMO model. The failure surfaces generated through MATLAB can be seen in Figure 11.

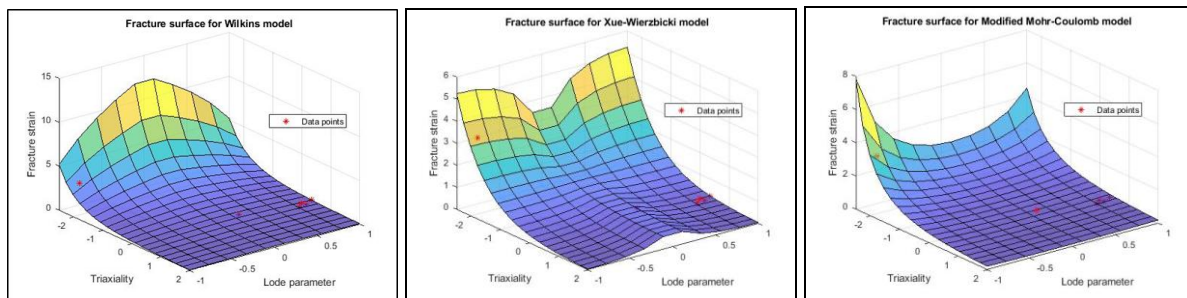


Fig.11: Failure surfaces: (from left to right) Wilkins, Xue-Wierzbicki, and Modified Mohr-Coulomb

5.3 Numerical Investigations

5.3.1 Joining Process Simulation

Since the joining process for SPR is performed using tools and fastener that are rotational symmetric about a central axis, the process simulation to predict the joint geometry is, therefore, performed through a 2D axisymmetric finite element model to save the computational effort. The punch, blank holder, and die are modelled as rigid parts while the rivet and sheets are treated as deformable parts. LS-DYNA is used as a numerical solver for this simulation.

The 2D joining process simulation was performed with the sheet material properties calculated from the unnotched specimen in the experimental program (without damage model) and the rivet material properties were used as received from the supplier. A displacement control was used for the movement of the punch. The *PART_ADAPTIVE_FAILURE option in LS-DYNA was used as the failure mechanism to model the piercing of top sheet by rivet. The other input parameters like friction, Remeshing frequency, mesh size, etc. were also optimized for the material combination. The final geometry of the simulation was compared with the picture of the micro-sectional cut of the joint from experiments and it matches quite well. The comparison is shown in Figure 12. The final joint geometry from process simulation was then carried over to perform the joint failure simulation.

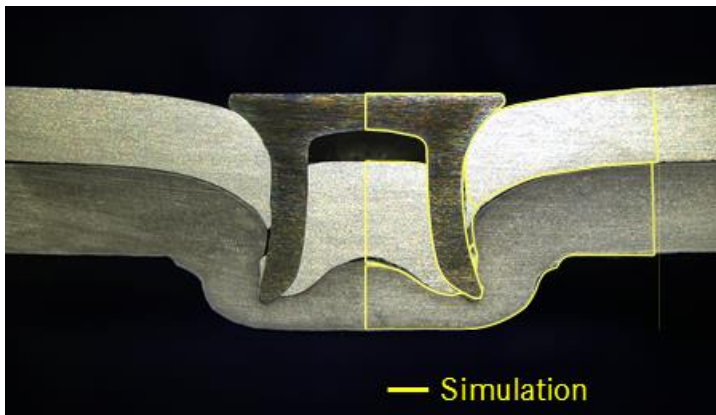


Fig.12: Comparison of final joint geometry from process simulation with geometry from experiment

5.3.2 Joint Failure Simulation

The analysis of the complex modes of joint failure under different loading conditions, as described in sub-section 2.1.2, requires detailed simulation models with solid elements to capture the through-thickness behavior of sheet materials accurately. The detailed models are generated from the results of previously described 2D axisymmetric process simulation. The methodology used for generation of inputs for joint failure simulation was discussed previously in section 4.

In this study, only the joint failure under shear loading with shear specimen (Figure 3) was considered for experimental and numerical studies. As mentioned in the previous sections, the joint failure simulation were first performed with readily available 2D damage/failure models: Gurson and GISSMO. The recently calibrated 3D damage models were then used for the joint failure analysis of the SPR joint during shear pull operation. The failure prediction mode for all the models was the same as V1. However, as compared to 2D Gurson and GISSMO models, the results with the calibrated damage models were closer to the experimental result as seen in Fig. 8.6, as the bottom sheet was deformed in a more similar fashion.

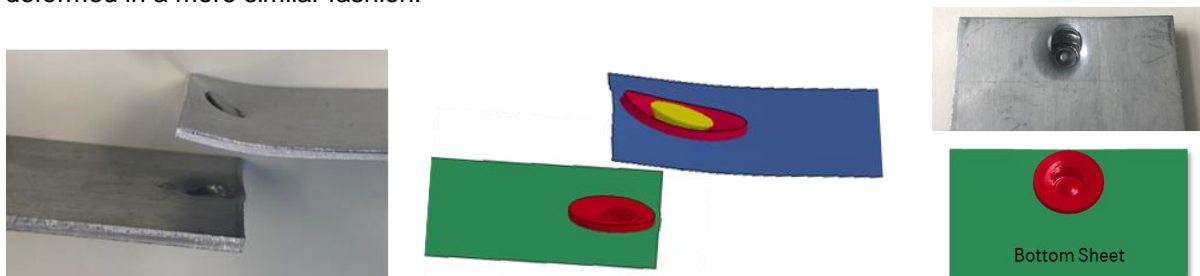


Fig.13: Simulation vs. Experiment: geometry after joint failure (Wilkins model)

On plotting the force-displacement curves and comparing them with the curves from experiments performed for shear loading of joints, it was observed that in terms of maximum force (indicating strength of SPR joint), the prediction with 2D Gurson model was a bit lower while the prediction with 2D GISSMO model was bit higher. The maximum force prediction with Wilkins and Xue-Wierzbicki models was almost similar and closest to the average experimental curve. With Modified Mohr-Coulomb model the maximum force predicted was a bit lower. A similar trend was observed for displacement at maximum force for all the investigated models. Out of the three 3D damage models, Wilkins model was found to be the overall best performing model by a close margin. The overall comparison of force-displacement curves can be seen in Figure 14 and 15. The worst case scenario was observed when the simulation was performed without any damage/failure model as the maximum force calculated was much higher and the displacement at maximum force is much lower than experiments. It can be seen that the overall shape of the curve for simulation without any damage/failure model exhibits a very stiff joint behavior under loading. The percentage deviations of maximum forces and displacements at maximum forces can be seen in Table 3.

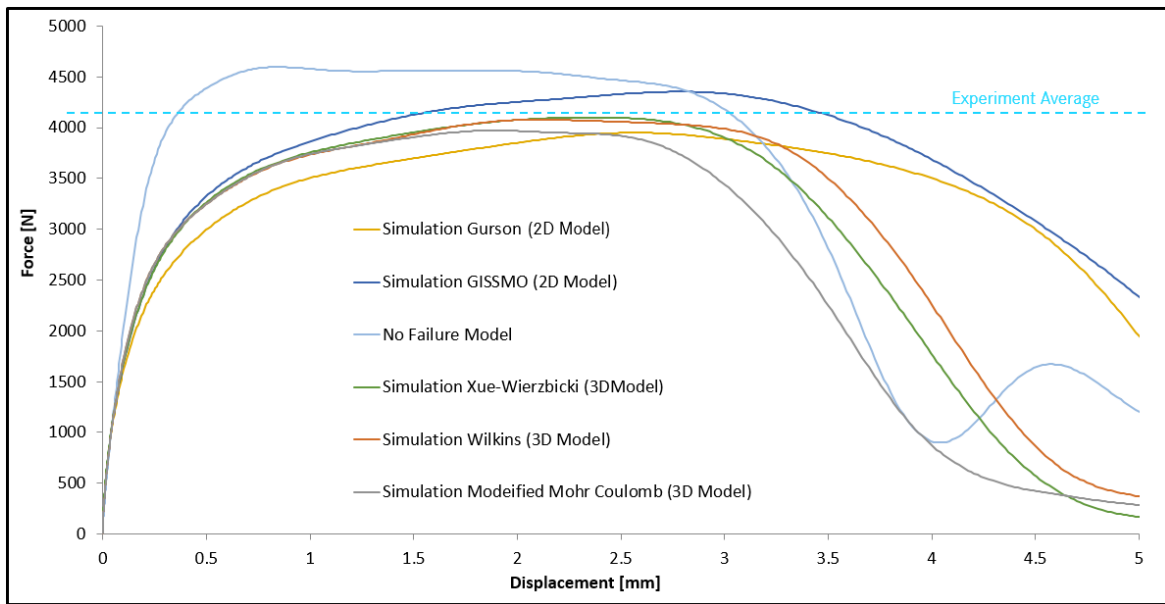


Fig.14: Comparison of force-displacement curves from all simulation variants

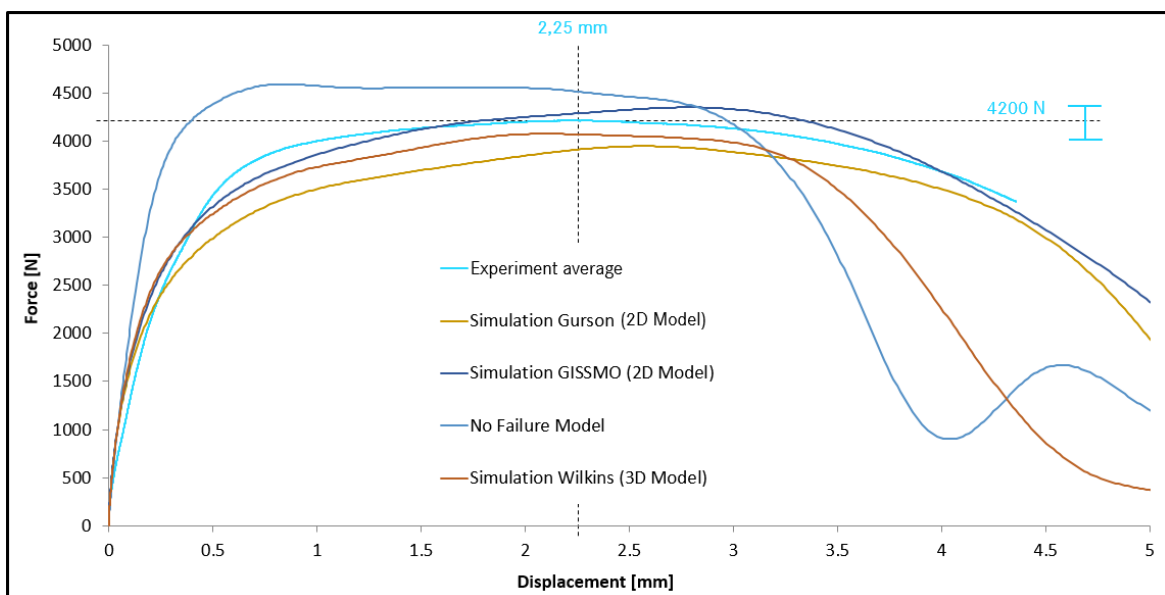


Fig.15: Comparison of force-displacement curves from all simulation variants (best from 3D damage models) with curve from experiment

Model	Deviation: Maximum Force	Deviation: Displacement at maximum force
Wilkins (3D Model)	- 2,3 %	- 5 %
GISSMO (2D Model)	+ 3,3 %	+ 33 %
Gurson (2D Model)	- 6,1 %	+ 10 %
No Failure Model	+ 10 %	- 65 %

Table 3: Percentage deviation of simulation results from experimental average value

6 Summary and Conclusion

The objective of this study was to perform finite element modelling of the Self-Piercing Riveting (SPR) joining process and to accurately predict the joint strength and failure in case of shear loading with the help of damage models. To fulfil the objective, a process chain was proposed which takes into consideration all the necessary steps involved in the simulation of SPR process flow in LS-DYNA. Since the failure in an SPR joint is always preceded by high deformation and/or fracture in either one or both sheet(s), a detailed joint failure model with solid elements was used to predict the failure mode accurately. For the numerical investigations with the detailed joint failure model, in addition to the already available 2D damage models: Gurson and GISSMO, three other damage models were chosen to be calibrated as 3D damage models: Wilkins, Xue-Wierzbicki, and Modified Mohr Coulomb. The calibration of models was performed by using the results from a comprehensive experimental program as inputs and with further optimizations on MATLAB. After the joining process simulation with the selected material combination, numerical investigations were performed with all the selected damage/failure models and the simulation results were compared with the experimental results from physical shear loading tests. The mode of failure was predicted correctly by all the damage models, however, the deformation pattern in bottom sheet was more accurately predicted by 3D damage models. The similar trend was observed while comparing the force-displacement curves from simulations and experiments.

In conclusion, the proposed simulation process chain performs adequately and can be used to predict the joint strength for any new material combinations with minimum experimental effort. Also the available crash material models (2D damage models) can be used for joint failure simulation but the 3D damage models are recommended because of their higher accuracy of prediction.

7 Literature

- [1] D. Li, A. Chrysanthou, I. Patel, and G. Williams: "Self-piercing riveting-a review," *International Journal for Advanced Manufacturing Technology*, 2017, p. 1777–1824.
- [2] R. Porcaro, A. Hanssen, M. Langseth, and A. Aalberg: "The behaviour of a selfpiercing riveted connection under quasi-static loading conditions", *International Journal of Solids and Structures*, 2006, p. 5110–5131.
- [3] P.-C. Lin, Z.-M. Su, W.-J. Lai, and J. Pan: "Fatigue behavior of self-piercing rivets and clinch joints in lap-shear specimens of aluminum sheets", *SAE Int. J. Mater. Manf*, 2013, doi: 10.4271/2013-01-1024.
- [4] T. L. Anderson: *Fracture Mechanics - Fundamentals and Applications – Third Edition*. Taylor & Francis, 2008.
- [5] T. S. Cao: "Models for ductile damage and fracture prediction in cold bulk metal forming processes: a review", *Int J Mater Form*, no. 10, 2017, p. 139–171.
- [6] L. Xue: "Ductile fracture modeling - theory, experimental investigation and numerical verification", Ph.D. dissertation, Massachusetts Institute of Technology, 2007.
- [7] F.J.P. Reis, F.X.C. Andrade: "Implementation and Application of a new Plasticity Model in LS-DYNA including Lode Angle Dependency", 11th German LS-DYNA Forum, 2012
- [8] M. Basaran: "Stress state dependent damage modeling with a focus on the lode angle influence", Ph.D. dissertation, RWTH Aachen, 2011
- [9] Gurson: "Continuum theory of ductile rupture by void nucleation and growth, part I – yield criteria and flow rules for porous ductile media", *J Engng Mater Technol*, no. 99, 1977, p. 2–15.
- [10] V. Tvergaard and A. Needleman: "Analysis of the cup-cone fracture in a round tensile bar", *Acta Metallurgica*, no. 32(1), 1984, p. 157–169.
- [11] F. Neukamm, M. Feucht, and A. Haufe: "Considering damage history in crashworthiness simulations", in *The 7th European LS-DYNA Conference*, Salzburg, Austria, 2009.
- [12] F. Neukamm, M. Feucht, and A. Haufe: "Consistent damage modelling in the process chain of forming to crashworthiness simulations", in *The 7th German LS-DYNA Conference*, vol. 30, Bamberg, Germany, 2009.
- [13] F. Neukamm, M. Feucht, and M. Bischoff: "On the application of continuum damage models to sheet metal forming simulations", in *X International Conference on Computational Plasticity*, CIMNE, Barcelona, Spain, 2009.
- [14] M. Wilkins, R. Streit, and J. Reaugh: "Cumulative-strain-damage model of ductile fracture: Simulation and prediction of engineering fracture tests", Lawrence Livermore National Laboratory, UCRL- 53058, 1980.
- [15] Y. Bao and T. Wierzbicki: "On fracture locus in the equivalent strain and stress triaxiality space", *Int. J. Mech. Sci.*, no. 46(1), 2004, p. 81–98.
- [16] L. Xue: "Damage accumulation and fracture initiation in uncracked ductile solids subject to triaxial loading", *International Journal of Solids and Structures*, no. 44, 2007, p. 5163–5181.
- [17] L. Xue: "Stress based fracture envelope for damage plastic solids", *Eng. Fract. Mech.*, no. 76(3), 2009, p. 419–438.
- [18] C. Coulomb: "Essai sur une application des regles des maximis et minimis a quelques problemes de statique relatifs al'architecture", *Mem Acad Roy des Sci*, 1776.
- [19] O. Mohr: "Abhandlungen aus dem Gebiete der technischen mechanik", 2nd ed. Berlin: Ernst, 1914.
- [20] LS-DYNA® KEYWORD USER'S MANUAL, VOLUME II: Material Models, R10.0, 2017
- [21] T. Wierzbicki, Y. Bao, Y. Lee, and Y. Bai: "Calibration and evaluation of seven fracture models", *Int J Mech Sci*, no. 47(4–5), 2005, p. 719– 743.
- [22] X. Zhuang, T. Wang, X. Zhu, and Z. Zhao: "Calibration and application of ductile fracture criterion under non-proportional loading condition", *Engineering Fracture Mechanics*, no. 165, 2016, p. 39–56.
- [23] H. Godhwani: "Innovative joining technique simulation for the digital development of the future", Master Thesis, Technische Universität Braunschweig, 2019